

Fabrication of a Graphene-Based Electrochemical Immunosensor for Ultrasensitive Analysis of Carcinoembryonic Antigens

Qingjun Cui^{*}

Clinical Laboratory, Xintai People's Hospital, Xintai, Shandong, 271200 P.R. China

*E-mail: qingjuncuiXPHX@163.com

Received: 14 June 2017 / *Accepted:* 13 August 2017 / *Published:* 12 September 2017

The clinical diagnosis and treatment evaluation of cancers require significantly sensitive determination of carcinoembryonic antigens (CEAs). This study proposed an electrochemical aptasensor for selective and sensitive determination of CEAs based on Pt/Au-diaminonaphthalene (DN)-graphene with the functions of electrocatalysts and nanocarriers. The capture of the developed bioconjugate onto the electrode surface occurred after the addition of CEAs via “sandwich” routes, which led to the appearance of an electrochemical response. An increase in the electrochemical response could be observed and ascribed to the desirable capacity, and peroxidase mimics the activity of dendritic Pt/Au/DN-graphene, where the reduction of H₂O₂ added to the electrolyte cell was catalysed. Therefore, the sensitivity of the as-prepared aptasensor could be enhanced herein.

Keywords: Carcinoembryonic antigen; Aptamer; Graphene; Immunosensor; Au NPs; Pt NPs

1. INTRODUCTION

Early clinical diagnosis of cancer is extremely essential to achieve a higher survival rate. Tumour markers are produced by cancer related-tumours and exist in host body fluids or tumour cells as macromolecules. The sensitive determination of tumour markers has been confirmed to be extremely important to the early determination of cancer and the monitoring of cancer recurrence [1, 2]. Recently, enzyme-linked immuno-sorbent assay (ELISA) [3, 4], chemiluminescence [5, 6], mass spectrometric immunoassays [7, 8] and many other immunoassays towards tumour markers have been proposed. Electrochemical immunosensors are portable and rapid in response time and require simple devices and thus have been especially attractive [9-12]. Nevertheless, recently proposed immunosensors usually suffer from long determination time, undesirable stability and sensitivity, and

complex determination procedures. For example, many immunosensors depend on two or three protocols to amplify the signal for further enhancement in sensitivity [13, 14]. Polymer entrapment, nanomaterial adsorption and covalent reaction used for the immobilization of the antibodies have the drawbacks of undesirable activity or unfavourable long-term stability and may lead to poor determination efficiency. Moreover, since macromolecule diffusion is low, there must be a long period of incubation.

Gold nanoparticles (AuNPs) could function as catalysts to not only promote the electrochemical reaction rate but also enhance the electron exchange between redox centres in biomolecules and electrode surfaces [15, 16]. Hence, AuNPs have been attractive in the fabrication of DNA–AuNP assemblies [17], enzyme biosensors [18], immunosensors [19, 20] and other electrical sensors. Diverse techniques and routes have been proposed to further promote the sensitivity of AuNP label-based immunosensors [21, 22]. In contrast to gold colloids, there was a surface plasmon band ranging between ~ 390 and 420 nm obtained for colloidal Ag nanoparticles (AgNPs), and the extinction coefficient was larger than that of AuNPs of the same size [23]. The nanoparticles with a core–shell structure have gained wide application in the immobilization and investigation of macromolecules, including proteins, enzymes, antibodies, and nucleotides and organ, tissue, and tumour in hyperthermia as a cytochemical label and matrix [24–26].

Highly ordered mesoporous carbon, carbon nanofibres, carbon nanotube and other carbon-based nanomaterials have gained wide application in the fabrication of diversely modified electrodes, since carbon nanotubes were discovered in 1991 [27]. In recent years, as a flat monolayer of carbon atoms tightly packed into a two-dimensional honeycomb lattice, graphene sheet (GS) possesses excellent features including desirable fracture strength, favourable conductivity and large specific surface area and has promoted a wide range of studies [28]. Hence, GS is a potential substitute to be applied in fields including biosensors, polymer composites and energy-storage materials [29–31].

In this study, an electrochemical immunosensor was fabricated through the immobilization of primary antibody (Ab_1) and the labelling of the secondary antibody (Ab_2) realized by the preparation of GS. To immobilize Ab_1 , the selected molecule 1,5-diaminonaphthalene (DN) was adsorbed onto GS via π – π stacking, which was employed to coat AuNPs and form a conjugated complex between AuNPs and Ab_1 . Moreover, DN was adsorbed onto GS, with the amino group of DN to coat Pt/Au nanoparticles and conjugate Ab_2 to prepare the tracer for Ab_2 labelling. An ultrasensitive immunosensor was fabricated under sandwich tactics with a model analyte of carcinoembryonic antigen (CEA).

2. EXPERIMENTS

2.1. Chemicals

L-Cysteine (L-Cys), thrombin (TB), human IgG, bovine serum albumin (BSA, 96–99%), chloroplatinic acid (H_2PtCl_6), gold chloride ($HAuCl_4$), toluidine blue (Tb) and carcinoembryonic antigen (CEA) were commercially available from Sigma Chemical Co. Acetone, ethylene glycol and hydrazine hydrate ($N_2H_4 \cdot H_2O$) were commercially available from Beijing Chemical Reagent Co.

(Beijing, China). Ascorbic acid (AA), diaminonaphthalene (DN), ethylenediamine tetraacetic sodium salt (EDTA) and polyvinylpyrrolidone (PVP) were commercially available from Chengdu Kelong Chemical Reagent Company (Chengdu, China). Sodium tellurite (Na_2TeO_3) was commercially available from Aladdin Industrial Corporation.

2.2. Preparation of Au/DN-graphene and Pt/Au/DN-graphene nanocomposites

Au nanoparticles were synthesized based on the literature [32]. The mixture of water (99 mL) and HAuCl_4 solution (1 mL, 1%) was heated to 97 °C. This was followed by the quick addition of trisodium citrate solution (10 g/L, 5 mL) through vigorous stirring. The mixed solution was heated for 10 min. Au colloid was then yielded after cooling the solution to ambient temperature under vigorous stirring. Graphene oxide (GO) was synthesized based on modified Hummer's method [33]. GO was then reduced by the reducing agent NaBH_4 at 85 °C for 3 h to obtain graphene [34]. The synthesis of DN-graphene began with the homogenous dispersion of DN (20 mg) and graphene (60 mg) into ethanol–water solution (60 mL, 1:1) under constant stirring at 25 °C for 48 h. After centrifugation and washing three times with ethanol and water, a black powder was yielded and dried in a vacuum at 60 °C for 1 d (denoted as Au/DN-graphene). Subsequently, the mixed solution of 200 mL of AuNPs and DN-graphene nanocomposites (30 mg) was vigorously stirred for 12 h and centrifuged to obtain the AuNP-enwrapped DN-graphene. After complete washing using deionized water, this nanocomposite was dried in a vacuum oven at 60 °C for 1 d.

The Au/DN-graphene (4 mL) and PVP (60 mg) were added to water (30 mL) and magnetically stirred for 10 min. This was followed by the quick injection of H_2PtCl_6 (1.6 mL; w/w, 1%) to the aforementioned suspension, to which was added AA (2 mL, 0.1 M). These reagents reacted in a water bath at 60 °C for 120 min to obtain a precipitate. After centrifugation, repeated washing using distilled water and dispersion for another period in water (3 mL), the dendritic Pt/Au/DN-graphene was yielded and stored in a refrigerator at 4 °C before use.

2.3. Preparation of secondary aptamer bioconjugate

A solution obtained after the injection of $\text{CEA}_{\text{apt}2}$ (400 μL , 2.5 μM) in pH 7.4 Tris–HCl buffer and Tb (3 mM, 100 μL) to the as-prepared Pt/Au/DN-graphene (1 mL) was left under stirring overnight below 4 °C, leading to the attachment of thiol-terminated $\text{CEA}_{\text{apt}2}$ and Tb containing – NH_2 groups to the dendritic Pt/Au/DN-graphene via Pt–S and Pt–N bonds, respectively (denoted $\text{CEA}_{\text{apt}1}/\text{Pt}/\text{Au}/\text{DN-graphene}/\text{GCE}$). This was followed by adding BSA (50 μL , w/w, 1%) to the mixed solution, which was stirred for 0.5 h to block the unoccupied active sites of Pt/Au/DN-graphene (denoted $\text{BSA}/\text{CEA}_{\text{apt}1}/\text{Pt}/\text{Au}/\text{DN-graphene}/\text{GCE}$). Further centrifugation and another suspension in water (1 mL) yielded the terminal bioconjugate, Pt/Au/DN-graphene– $\text{CEA}_{\text{apt}2}$ –Tb. All aforementioned tests were carried out at 4 °C. In addition, Au/DN-graphene– $\text{CEA}_{\text{apt}2}$ –Tb bioconjugate in the absence of Pt was prepared through a similar process for the control experiment (denoted $\text{CEA}/\text{BSA}/\text{CEA}_{\text{apt}1}/\text{Pt}/\text{Au}/\text{DN-graphene}/\text{GCE}$).

2.4. Fabrication of the immunosensor

After careful polishing using Al_2O_3 powder (0.3 μm and 0.05 μm , successively), the original GCE was washed using ethanol and double distilled water under ultrasonication. This was followed by the electrodeposition of gold nanoparticles (AuNPs) onto the as-prepared GCE 1% w/w HAuCl_4 solution for 0.5 min (potential: -0.2 V). Subsequently, CEA_{apt1} was successfully immobilized via Au–S affinity after dropping CEA_{apt1} (2.5 μM , 20 μL) in pH 7.4 Tris–HCl buffer onto the decorated surface of the electrode at ambient temperature for 18 h. The terminal electrode was then incubated in BSA (w/w, 1%; 20 μL) for 40 min for the blocking of the residual active sites and the elimination of the non-specific binding effects. This was followed by coating proper concentrations of CEA standard solution (20 μL) on the terminal electrode at ambient temperature for 40 min. Pt/Au/DN-graphene– CEA_{apt2} –Tb (20 μL) was then incubated for another 60 min. Finally, the sandwich-type aptasensor was rinsed using distilled water and stored at 4 $^\circ\text{C}$ before further use.

3. RESULTS AND DISCUSSION

Initially, CV measurements were carried out in $\text{K}_3[\text{Fe}(\text{CN})_6]/\text{K}_4[\text{Fe}(\text{CN})_6]$ (5 mM) at a scan rate of 100 mV/s to characterize the preparation of our developed aptasensor, as shown in Fig. 1. The original GCE displayed a reversible CV profile. As HAuCl_4 (w/w, 1%) was electrodeposited, an increase in the peak current was observed, due to the potential promotion of the electron exchange by the conductive nano-Au. The peak current decreased as soon as CEA_{apt1} was immobilized, suggesting the hindrance of the electron exchange channel by CEA_{apt1} .

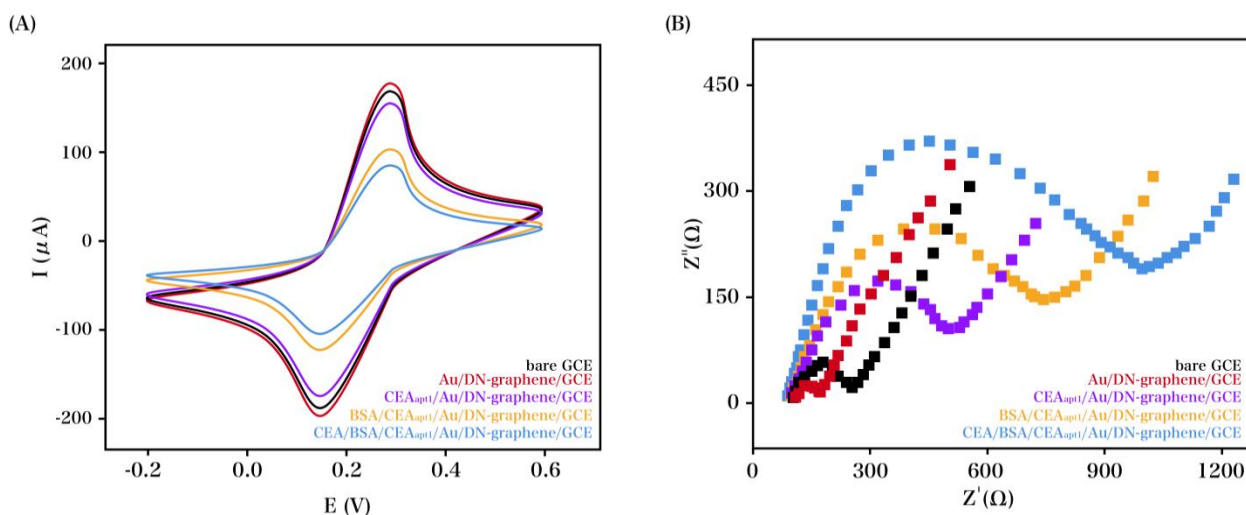


Figure 1. (A) CV and (B) EIS patterns of the stepwise decorated electrode in $\text{K}_3[\text{Fe}(\text{CN})_6]/\text{K}_4[\text{Fe}(\text{CN})_6]$ (5 mM). The scan rate of CV is 50 mV/s (2.5 μM CEA_{apt1} and 10 ng/mL CEA incubated for 40 min).

This phenomenon was attributed to the electronically inert property of protein that could block the electron transfer at the modified GCE [35]. There was a further decrease in the peak current of the

electrochemical response upon the immobilization of the non-conductive BSA onto the surface of the terminal electrode. By measuring the change of electron transfer resistance during the biorecognition on the electrode surface, CV can also be utilized as an efficient analytical system to monitor the interfacial properties of highly biospecific recognition in the presence of the analytes [36]. A decrease in the peak current was observed after CEA (10 ng/mL) was added, suggesting that the CEA_{apt1}-CEA complex formed on the surface of the terminal electrode and thus that the block layer became inert and the electron exchange was hindered.

The interface features of surface-decorated electrodes were further validated by means of electrochemical impedance spectroscopy (EIS). There was an extremely small semicircular region observed at the original GCE (Fig. 1B), which became smaller after HAuCl₄ (w/w, 1%) was electrodeposited. This variation indicated that the nano-Au was more conductive. Nevertheless, a pronounced increase in the semicircle diameter was observed after the CEA_{apt1} was immobilized, suggesting the blocking of the electron exchange channel by the existing CEA_{apt1}. The semicircle diameter further increased upon use of inert BSA to block the residual active sites, indicating that BSA hindered the electron exchange. After the incubation of the terminal aptasensor using CEA (10 ng/mL), a further increase in the semicircle diameter was observed since the CEA_{apt1}-CEA complex formed and hindered the electron exchange channel. Therefore, the proposed immunosensor is meaningful for CEA quantitative analysis in clinical applications. Characteristics such as the detection method, linear range and detection limit achieved in other electrochemical immunosensors were further studied.

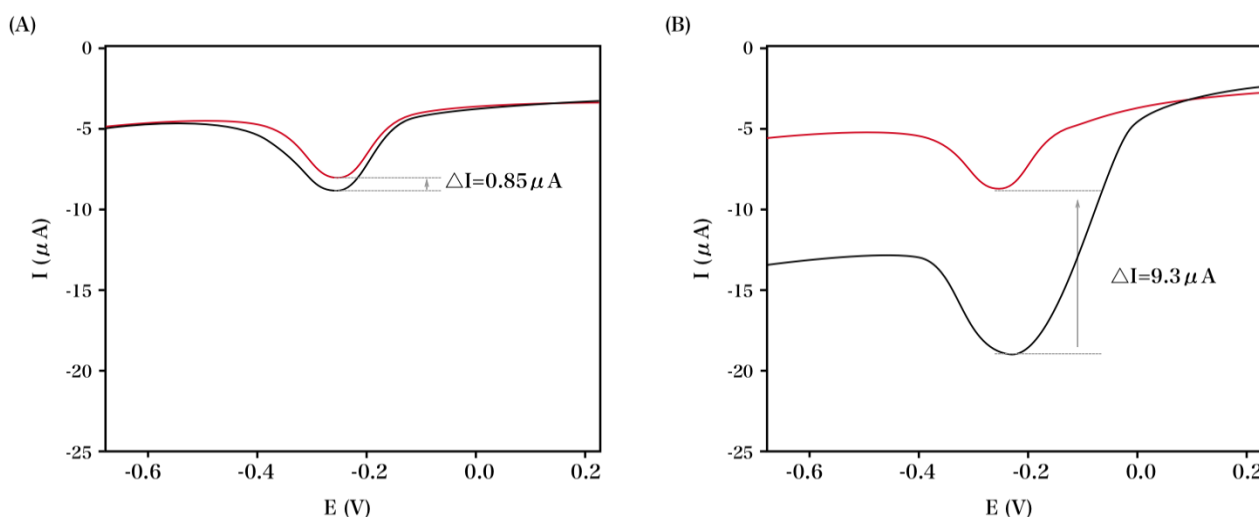


Figure 2. DPV responses of our developed aptasensor after incubation with CEA_{apt1} (2.5 μM), CEA (10 ng/mL) and two secondary aptamer bioconjugates: (A) Au/ND-graphene-CEA_{apt2}-Tb and (B) Pt/Au/ND-graphene-CEA_{apt2}-Tb, then assayed in 0.1 M of PBS (pH 7.0) before and after the addition of H₂O₂ (0.8 mM).

The comparison of the electrochemical response using Pt/Au/ND-graphene-CEA_{apt2}-Tb and Au/DN-graphene-CEA_{apt2}-Tb was studied under optimal test conditions to show the catalytic capacity of Pt/Au/DN-graphene in our developed bioconjugate. The formed antigen-antibody immunocomplex

on the electrode surface hindered the electron transfer towards the electrode surface, resulting in a decrease of the electrochemical signal [37]. With the immobilization of the proposed aptasensor using Au/ND-graphene- $\text{CEA}_{\text{apt}2}$ -Tb and CEA (10 ng/mL), there was a slight DPV response increase as H_2O_2 (0.8 mM) was added to PBS (1 mL) (Fig. 3A). However, there was an obvious increase in DPV response upon using our developed bioconjugate before and after the addition of H_2O_2 (0.8 mM) to PBS (1 mL), as shown in Fig. 2B. The electrochemical amplification capacity of our developed bioconjugate (over 9 times) was possible due to the excellent catalytic behaviour of Pt/Au/ND-graphene, which possessed desirable catalytic activity towards the reduction of H_2O_2 . Thus, the acceleration of the electron exchange of Tb would be facilitated, and the electrochemical response would increase. Hence, our developed aptasensor has the potential to be more sensitive, thereby providing remarkable analytical behaviour for the fabrication of a determination platform for CEA.

The electrochemical response of a Pt/Au/ND-graphene-based CEA aptasensor is investigated in PBS (1 mL) + H_2O_2 (0.8 mM) under optimal test conditions to evaluate its quantitative analysis capability. The aptasensor incubated using CEA with different concentrations is characterized via DPV profiles (Fig. 3A), along with the calibration relationship of DPV peak current using CEA at different concentrations. As the concentration of CEA increased (0.001 ng/mL to 80 ng/mL), an increase in the current response was observed, since the increase in CEA at the electrode surface led to the combination of an increasing number of Pt/Au/ND-graphene- $\text{CEA}_{\text{apt}2}$ -Tb bioconjugates via a specific sandwich-type reaction among $\text{CEA}_{\text{apt}1}$, CEA and $\text{CEA}_{\text{apt}2}$. At the same time, the DPV signal was found to be linearly related to the logarithm of CEA concentration. The LOD of the as-prepared aptasensor was 0.32 pM, as calculated by a previous technique [38].

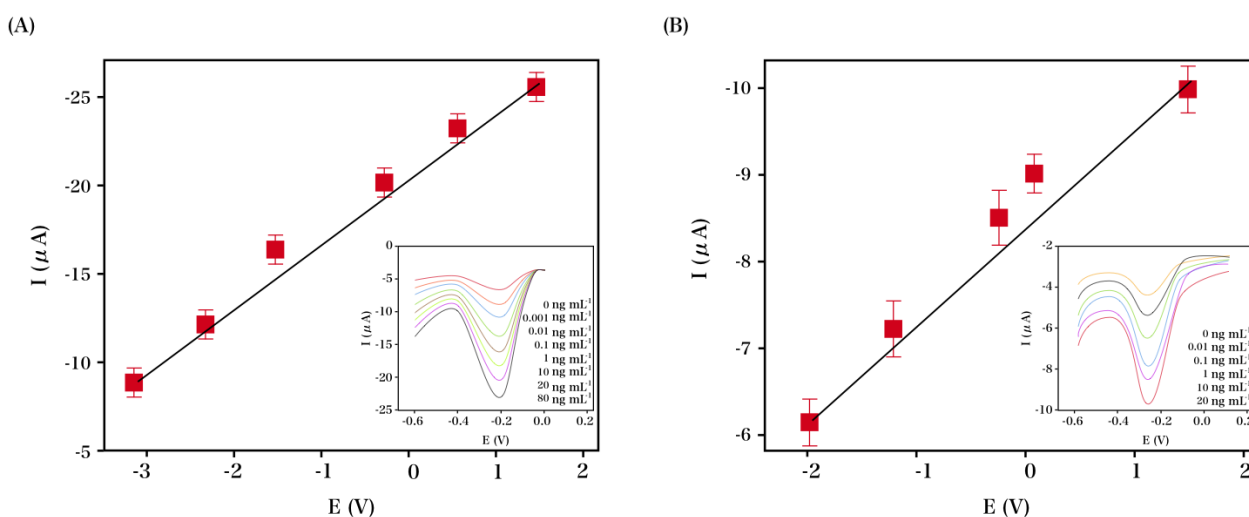


Figure 3. The calibration plot of the DPV peak current vs. CEA concentrations using different secondary aptamer bioconjugates: (A) Pt/Au/ND-graphene- $\text{CEA}_{\text{apt}2}$ -Tb and (B) Au/ND-graphene- $\text{CEA}_{\text{apt}2}$ -Tb. DPV profiles of our developed aptasensor towards CEA at varied concentrations are shown in the insets.

The response for each concentration was the average response of the immunoreaction with the corresponding standard deviation of triplicate analytical cycles. As shown in Fig. 3B, the DPV peak

current for CEA with only Au/ND-graphene amplification was characterized via the calibration plot. Au/ND-graphene displayed poorer sensitivity and a less desirable dynamic linear range than dendritic Pt/Au/ND-graphene used for signal enhancement, where the electrocatalytic activity to H_2O_2 reduction became enhanced and the amplification capacity to the electrochemical response became more obvious due to dendritic Pt/Au/ND-graphene. Moreover, the Pt/Au/ND-graphene- CEA_{apt2} -Tb bioconjugate-based aptasensor was compared with DPV, surface-enhanced Raman scattering (SERS), electrochemiluminescence (ECL), cyclic voltammetry (CV), chemiluminescence (CL) and other techniques in their analytical behaviour, as shown in Table 1. According to the results, the dendritic Pt/Au/ND-graphene(signal enhancer)-based detection sensor was found to be analytically sensitive, with a detectable concentration range to CEA, thus indicating that the proposed aptasensor was simple, cost-effective, and applicable in real specimen detection.

The electrochemical response of L-Cys, thrombin (TB), alpha fetoprotein (AFP), human IgG and other interfering agents was studied in PBS (1 mL) + H_2O_2 (0.8 mM) to measure the specificity of our developed aptasensor. During the respective determination of human IgG, L-Cys, AFP and TB (100 ng/mL), there was no pronounced DPV response signal. By comparison, the as-prepared bioconjugate before and after the addition of the aforementioned interfering agents (100 ng/mL) displayed an obvious DPV response signal towards the target CEA (10 ng/mL), indicating that the Pt/Au/ND-graphene- CEA_{apt2} -Tb-based CEA aptasensor was desirably specific. This could be explained by the excellent catalytic activity of Pt/Au/ND-graphene and desirable electrochemical response increase. The study was performed by measuring the interference with and without CEA.

Table 1. Comparisons between our developed aptasensor and other routes.

Methods	Linear range (pg/mL)	Detection limit (pg/mL)	Reference
CL	654-6540	8	[39]
CV	2-80000	1	[40]
ECL	10-10000	3.8	[41]
Colorimetry	50-5000	48	[42]
SERS	1-10000	1	[43]
DPV	500-25000	220	[44]
DPV	10-12000	5	[45]
Proposed sensor	1-80000	0.32	This work

Four aptasensors were incubated in 10 ng/mL CEA under the same conditions, with their electrochemical response obtained to study the reproducibility of the as-prepared aptasensor. The electrochemical signal was confirmed to be reproducible with a relative standard deviation (RSD) of 5.1%, suggesting that the as-prepared sensor was desirably reproducible. In addition, the as-prepared aptasensor was incubated with CEA (10 ng/mL) in PBS (1.07 mL) + H_2O_2 (0.8 mM) and stored at 4 °C for 10 days, to investigate the stability of this aptasensor. The DPV peak current was found to retain 94.4% of its initial current, suggesting that the Pt/Au/ND-graphene- CEA_{apt2} -Tb-based aptasensor was desirably stable. Clinical serum samples were collected from The Xintai People's Hospital for further

investigation of the analytical reliability and potential application of the as-prepared technique in real specimen detection.

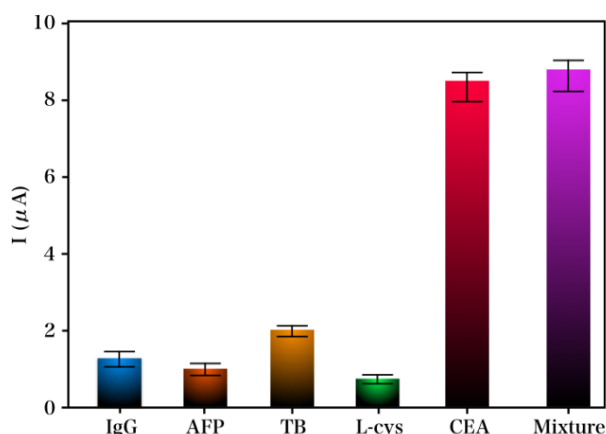


Figure 4. Comparison of specificity towards 10 ng/mL target CEA using the developed aptasensor and other interfering agents including L-Cys, TB, AFP, IgG before and after the addition of CEA (10 ng/mL).

This work compared the measurement results of CEA in human serum specimens obtained by our developed technique with the reference values using the purchased Electrochemiluminescent Analyzer (ROCHE E601, Switzerland). As showed in Table 2, relative errors were observed below 5.44% for the determination of CEA, with a recovery range of 94.7% to 104.2% for the CEA recovery test. These acceptable results indicated that our developed technique was accurate for the specimen determination.

Table 2. Application of the aptasensor in real specimens.

Sample	Added (pg/mL)	Found (pg/mL)	RSD (%)	Recovery (%)	Reference value (pg/mL)
1	200	215	3.22	107.5	205
2	500	488	1.06	97.6	503
3	1000	963	5.44	96.5	977
4	2000	2077	2.67	103.85	1968

4. CONCLUSIONS

In this work, the Pt/Au/ND-graphene-CEA_{apt2}-Tb bioconjugate was synthesized to fabricate a sandwich-type electrochemical aptasensor for selective and sensitive CEA detection. Both the electron exchange and electrochemical response signal could be promoted due to the desirable conductivity and peroxidase mimicking activity of dendritic Pt/Au/ND-graphene, where the reduction of H₂O₂ added to

the electrolyte cell was catalysed. Therefore, both the sensitivity and analytical behaviour of the as-prepared aptasensor could be enhanced.

References

1. H. Kitano, *Science*, 295 (2002) 1662.
2. P.R. Srinivas, B.S. Kramer and S. Srivastava, *The lancet oncology*, 2 (2001) 698.
3. A. Voller, A. Bartlett and D. Bidwell, *Journal of Clinical Pathology*, 31 (1978) 507.
4. A.M. Yates, S.J. Elvin and D.E. Williamson, *Journal of immunoassay*, 20 (1999) 31.
5. Z. Fu, C. Hao, X. Fei and H. Ju, *Journal of immunological methods*, 312 (2006) 61.
6. Z. Fu, F. Yan, H. Liu, Z. Yang and H. Ju, *Biosensors and Bioelectronics*, 23 (2008) 1063.
7. E.E. Niederkofler, K.A. Tubbs, K. Gruber, D. Nedelkov, U.A. Kiernan, P. Williams and R.W. Nelson, *Anal. Chem.*, 73 (2001) 3294.
8. S. Hu, S. Zhang, Z. Hu, Z. Xing and X. Zhang, *Anal. Chem.*, 79 (2007) 923.
9. J. Tang, D. Tang, B. Su, Q. Li, B. Qiu and G. Chen, *Electrochimica Acta*, 56 (2011) 8168.
10. S. Guo, D. Wen, Y. Zhai, S. Dong and E. Wang, *Biosensors and Bioelectronics*, 26 (2011) 3475.
11. X. Luo, Q. Xu, T. James and J.J. Davis, *Anal. Chem.*, 86 (2014) 5553.
12. H. Kalso, N. Inguibert, L. Barthelmebs, G. Istamboulie, F. Thomas, C. Calas-Blanchard and T. Noguier, *Chemical Communications*, 50 (2014) 1658.
13. D. Du, Z. Zou, Y. Shin, J. Wang, H. Wu, M.H. Engelhard, J. Liu, I.A. Aksay and Y. Lin, *Anal. Chem.*, 82 (2010) 2989.
14. B. Kavosi, A. Salimi, R. Hallaj and K. Amani, *Biosensors and Bioelectronics*, 52 (2014) 20.
15. V. Mani, B.V. Chikkaveeraiah, V. Patel, J.S. Gutkind and J.F. Rusling, *ACS nano*, 3 (2009) 585.
16. P.S. Jensen, Q. Chi, F.B. Grummen, J.M. Abad, A. Horsewell, D.J. Schiffrin and J. Ulstrup, *J Phys Chem C*, 111 (2007) 6124.
17. H. Shu, W. Wen, H. Xiong, X. Zhang and S. Wang, *Electrochemistry Communications*, 37 (2013) 15.
18. A. Singh, S. Park and H. Yang, *Anal. Chem.*, 85 (2013) 4863.
19. G. Yang, L. Li, R.K. Rana and J.-J. Zhu, *Carbon*, 61 (2013) 357.
20. D. Lin, J. Wu, H. Ju and F. Yan, *Biosensors and Bioelectronics*, 52 (2014) 153.
21. T. Xu, X. Jia, X. Chen and Z. Ma, *Biosensors and Bioelectronics*, 56 (2014) 174.
22. G.-X. Zhong, P. Wang, F.-H. Fu, S.-H. Weng, W. Chen, S.-G. Li, A.-L. Liu, Z.-Y. Wu, X. Zhu and X.-H. Lin, *Talanta*, 125 (2014) 439.
23. S. Link, Z.L. Wang and M.A. El-Sayed, *Journal of Physical Chemistry B*, 103 (1999) 3529.
24. J. Li, Q. Xu, X. Wei and Z. Hao, *Journal of agricultural and food chemistry*, 61 (2013) 1435.
25. J. Wang, H. Han, X. Jiang, L. Huang, L. Chen and N. Li, *Anal. Chem.*, 84 (2012) 4893.
26. D. Tang, R. Yuan and Y. Chai, *J Phys Chem B*, 110 (2006) 11640.
27. M. Zhou, J. Ding, L.-p. Guo and Q.-k. Shang, *Anal. Chem.*, 79 (2007) 5328.
28. T. Ohta, A. Bostwick, T. Seyller, K. Horn and E. Rotenberg, *Science*, 313 (2006) 951.
29. L. Zhu, L. Xu, N. Jia, B. Huang, L. Tan, S. Yang and S. Yao, *Talanta*, 116 (2013) 809.
30. K. Shao, J. Wang, X. Jiang, F. Shao, T. Li, S. Ye, L. Chen and H. Han, *Anal. Chem.*, 86 (2014) 5749.
31. H.V. Tran, B. Piro, S. Reisberg, H.T. Duc and M.C. Pham, *Anal. Chem.*, 85 (2013) 8469.
32. P. Tartaj, T. González-Carreño and C.J. Serna, *Langmuir*, 18 (2002) 4556.
33. R. Muszynski, B. Seger and P.V. Kamat, *J Phys Chem C*, 112 (2008) 5263.
34. Y. Zhao, L. Zhan, J. Tian, S. Nie and Z. Ning, *Electrochimica Acta*, 56 (2011) 1967.
35. Y. Li, Y. Chen, D. Deng, L. Luo, H. He and Z. Wang, *Sensors and Actuators B: Chemical*, 248 (2017) 966.
36. J. Gao, Z. Guo, F. Su, L. Gao, X. Pang, W. Cao, B. Du and Q. Wei, *Biosensors and Bioelectronics*,

- 63 (2015) 465.
37. S. Samanman, A. Numnuam, W. Limbut, P. Kanatharana and P. Thavarungkul, *Analytica Chimica Acta*, 853 (2015) 521.
38. A.-E. Radi, J.L. Acero Sánchez, E. Baldrich and C.K. O'Sullivan, *Journal of the American Chemical Society*, 128 (2006) 117.
39. J.W. Park, W. Na and J. Jang, *RSC Advances*, 6 (2016) 14335.
40. B. Su, D. Tang, J. Tang, Y. Cui and G. Chen, *Biosensors and Bioelectronics*, 30 (2011) 229.
41. G.-F. Shi, J.-T. Cao, J.-J. Zhang, K.-J. Huang, Y.-M. Liu, Y.-H. Chen and S.-W. Ren, *The Analyst*, 139 (2014) 5827.
42. C. Gao, M. Su, Y. Wang, S. Ge and J. Yu, *Rsc Advances*, 5 (2015) 28324.
43. H. Chon, S. Lee, S.W. Son, C.H. Oh and J. Choo, *Anal. Chem.*, 81 (2009) 3029.
44. J. Wu, J. Tang, Z. Dai, F. Yan, H. Ju and N. El Murr, *Biosensors and Bioelectronics*, 22 (2006) 102.
45. Q. Li, D. Tang, J. Tang, B. Su, J. Huang and G. Chen, *Talanta*, 84 (2011) 538.

© 2017 The Authors. Published by ESG (www.electrochemsci.org). This article is an open access article distributed under the terms and conditions of the Creative Commons Attribution license (<http://creativecommons.org/licenses/by/4.0/>).